Journal of Geosciences, 69 (2024), 183–197 DOI: 10.3190/jgeosci.396

Original paper

Intrusions of coherent volcanic rocks as reason, why eroded diatremes may form positive topography: an example of Bídnice diatreme, Czech Republic

Martin ALEXA[1,2*], Jakub MYSLIVEČEK[1,2], Jan FRANĚK[1], Jan VALENTA[2,3], Zoltán PÉCSKAY[4]

[1] *Czech Geological Survey, Klárov 3, 118 21 Prague 1, Czech Republic; martin.alexa@geology.cz*
[2] *Faculty of Science, Charles University in Prague, Albertov 6, Prague, Czech Republic*
[3] *Institute of Rock Structure and Mechanics, Czech Academy of Sciences, V Holešovičkách 41, 182 09 Prague 8, Czech Republic*
[4] *Institute of Nuclear Research, Hungarian Academy of Sciences, Bem tér 18/c, Debrecen, Hungary*
**Corresponding author*

The Bídnice hill near Litoměřice, Czech Republic, has been recognized as a volcanic structure during a survey for a new railway connection between Prague and Dresden, where after several campaigns of combined geophysical survey, it has been concluded, that Bídnice is actually a deeply eroded peanut-shaped maar-diatreme volcano forming a positive morphology. The reason for the higher resistance of the disintegrated rock in the diatreme fill against the erosion when compared to surrounding country rocks was the main question of our presented research. While other positive-morphology diatremes in the region are mostly associated with high-viscosity differentiated alkaline rocks (namely phonolites), the Bídnice diatreme comprises intrusions of basic rock (SiO_2 ca 38 wt. %), classified as olivine nephelinite. From the geophysical survey of the internal structure, comprising magnetometry and electrical resistivity tomography, a spoon-like subsurface intrusions of the olivine nephelinite were found. A smaller outcrop of the intrusive system penetrating the diatreme provided a K–Ar age of 27.06 ± 0.57 Ma (Oligocene). The results of the geophysical survey were then used to create a 3D geological model to better understand and interpret the geological setting. A system of coherent sills, even with a rather low thickness in the case of low-viscosity (ultra)mafic rocks, may be responsible for the reinforcement of the diatreme leading in slower erosion, and therefore resulting in the significant positive topography of eroded maar-diatreme volcano. In addition, sub-horizontal intrusions provide more homogeneous reinforcement of the diatreme against erosion compared to subvertical dykes, those would be exposed by the selective erosion in the form of small ridges.

Keywords: Diatreme, intrusion, electrical resistivity tomography, České Středohoří Volcanic Complex, Bídnice hill
Received: 1 April 2023; accepted: 18 September 2024; handling editor: A. Guy
The online version of this article (doi: 10.3190/jgeosci.396) contains electronic supplementary material.

1. Introduction

Maar volcano is a form of low-relief volcanic crater most usually formed in a phreatomagmatic eruption caused by the contact of subsurface waters with rising magma (e.g., Németh et al. 2007; White and Ross 2011; White and Valentine 2016). The contact of hot magma with cold water results in immediate vaporization, leading to an explosion. When the strength limit with the gravity load of the overlying rocks is exceeded, an explosion occurs, during which the resulting tension is quickly released and the overlaying material is thrown out into the wider area around the maar crater. Maars are usually created by a series of explosions in rapid succession with a gradually deepening focus (White and Ross 2011), which causes the crater to deepen with each explosion. The pyroclastic ring encircling the crater is built of ejected pyroclasts, dominated by country-rock fragments over minor juvenile clasts. Maar volcanoes usually form a negative landform in topography, except for the maar-bounding pyroclastic ring. The deeper part of the funnel-shaped crater is filled with breccias of shattered country-rocks, known as diatremes. Despite the diatreme is filled with disintegrated country-rocks and therefore should be more prone to erosion, it may in many cases form hills (e.g., Németh et al. 2001, 2007; Fodor et al. 2005; Latutrie and Ross 2019; van Wyk de Vries et al. 2022; Hencz et al. 2024). How can an originally negative landform become positive, when the disintegrated rocks of the diatreme fill should weather and undergo erosion faster than the surrounding unaffected rocks?

With an aim to better understand the mechanisms controlling the inverted erosional rates exposing diatremes above the surrounding landscape, we focused on an example of a newly discovered diatreme at Bídnice hill near Litoměřice in northern Bohemia, which penetrates through a siliciclastic sequence of Cretaceous marine sediments. As fragments of basalt rock were found at a locality where

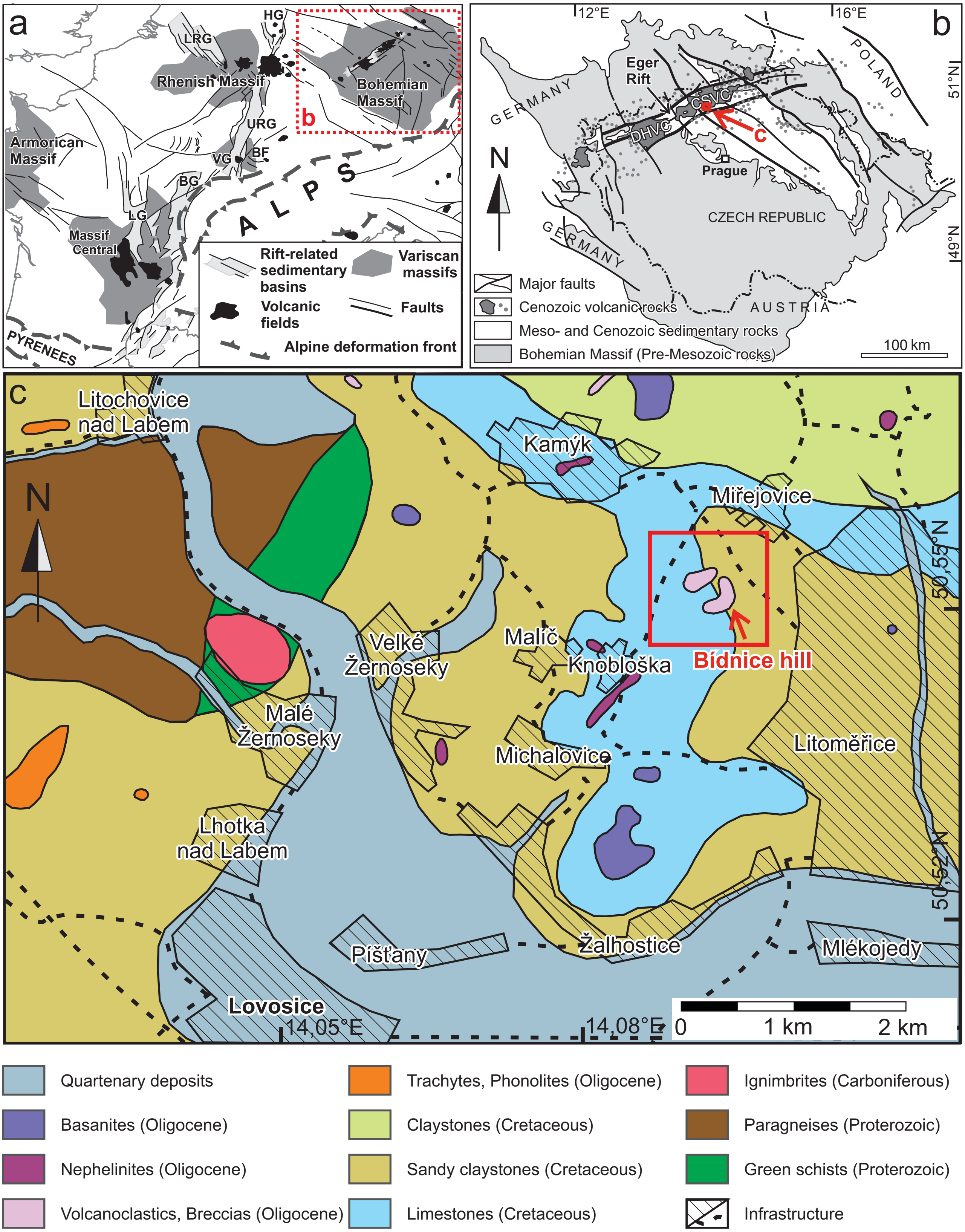

Fig. 1 a – location of the Bohemian Massif in European platform; **b** – location of Eger rift in Bohemian Massif and studied area within **c** – geological sketch-map of the study location and its surroundings. CSVC = České Středohoří Volcanic Complex, DHVC = Doupovské Hory Volcanic Complex.

only Cretaceous rocks were expected, the surrounding area was checked for outcrops and several of them expose volcanic breccia. In this case, however, the volcanic structure forms an inverted relief and is found on top of a hill. From geomorphology analysis combined with the outcrops and field mapping, it seems that there is a peanut-shaped (Graettinger and Bearden 2021) twinned diatreme.

Maar volcanoes are often subjects of geophysical research as it is usually the only possibility of imaging the internal structure of a diatreme and its feeding dykes. The diatreme breccia tends to be a significant source of negative gravity anomalies (e.g., Mrlina et al. 2009; Schulz et al. 2005; Skácelová et al. 2010; Hrubcová et al. 2023), low-resistivity anomalies (e.g., Hošek et al. 2019; Mrlina et al. 2009; Skácelová et al. 2010; Hrubcová et al. 2023) and low seismic velocity anomalies (e.g., Gebhardt et al. 2011), while the magmatic feeder is associated with magnetic anomalies (e.g., Valenta et al. 2014b; Hrubcová et al. 2023). A ground geophysical survey was thus conducted at the Bídnice diatreme to better understand the internal structure and to reveal the reason why this diatreme forms a hill, which may help to explain the inverted morphology of other diatremes worldwide.

2. Geological setting

Cenozoic volcanic activity manifested itself significantly throughout the Western and Central Europe and significantly affected the area of the Bohemian Massif. Within-plate alkaline volcanism in Western and Central Europe has been associated with a system of rift zones, mainly oriented north–south (Fig. 1a). This large-scale rift system formed as a remote response to the collision between the European and African lithospheric plates during the Paleogene (Wilson and Downes 1991; Goes et al. 1999; Ulrych et al. 1999; Wedepohl and Bauman 1999; Jung et al. 2011).

The magmatism of the Bohemian Massif represents the easternmost branch of the Central European Volcanic Province (CEVP of Wilson and Downes 1991; Hoernle et al. 1995; Ulrych et al. 1999, 2011; Lustrino and Wilson 2007). In the Czech Republic, the most significant magmatic activity of the Cenozoic period is bound to the Ohře (Eger) rift (Fig. 1b). The rift zone follows the NE–SW trending Variscan suture between the Teplá-Barrandian and Saxothuringian domains of the Bohemian Massif reactivated during the Alpine orogenesis (Babuška and Plomerová 1992, 2001, 2010; Mlčoch and Konopásek 2010). Along this tectonic line, a number of larger volcanic complexes were formed (but also many smaller scattered volcanic bodies) during the Cenozoic. The most important volcanic complexes in the area are the Doupovské Hory Volcanic Complex (e.g., Holub et al. 2010) and the České Středohoří Volcanic Complex (CSVC: Cajz et al. 1999, 2009; Ackerman et al. 2015).

The evolution of the CSVC lasted since the Late Eocene until the Late Miocene and its eruptive products represent sequence of four formations: (Cajz et al. 1999, 2009; Ulrych et al. 2002): basanitic Ústí Fm. (36.1–25.5 Ma), trachybasaltic Děčín Fm. (30.8–24.7 Ma), basanitic Dobrná Fm. (24.0–19.3 Ma), and basanitic Štrbice Fm. (13.9–9.0 Ma), respectively. The basaltic rocks are present in the form of lavas, dykes and conduits associated with various types of volcanoclastic rocks. The basaltic rocks are also accompanied by more differentiated alkaline rocks in the CSVC. According to Ackerman et al. (2015), the trachybasalts were derived from basanites of the Ústí Fm. though fractional crystallization and further fractionation associated with assimilation of crustal rocks produced trachytic and phonolitic magmas. This study focuses on the newly discovered volcanic diatreme of Bídnice hill, located approximately 2.8 km northwest of the center of Litoměřice town near the small settlement Knobloška (Fig. 1c). So far, this hill has been depicted as Cretaceous sedimentary rocks. Volcanic products intruded into clayey-glauconitic sandstones of the Jizera Formation (Middle to Upper Turonian), marlstones and limestones of the Teplice Formation (Upper Turonian to Lower Coniacian) and claystones to marlstones of the Březno Formation (Coniacian) of the Bohemian Cretaceous Basin (Domas 1988). The presence of coherent volcanic rocks and volcanic breccias was discovered in 2017 during the geological survey for the new railway connection of Prague with Dresden.

3. Methods

Ground geophysical methods represent an effective tool to visualise the internal unexposed structure of volcanic constructs, where different rocks with distinct physical properties alternate (e.g., Gebhardt et al. 2011; Hrubcová et al. 2023). Therefore, electrical resistivity tomography (ERT) and magnetic surveys were chosen to explore the subsurface structure, and hence also the origin of the Bídnice hill. The ground geophysical survey was conducted during several campaigns in July 2017, November 2021, March 2022 and September 2022 with an aim to achieve a dense network of data allowing reconstruction of the Bídnice diatreme internal structure. The measured data sets are available in the Electronic Supplementary Material (ESM).

3.1. Magnetometry

Unlike the surrounding Cretaceous sediments, the mafic volcanic rocks have a significant impact on the Earth's

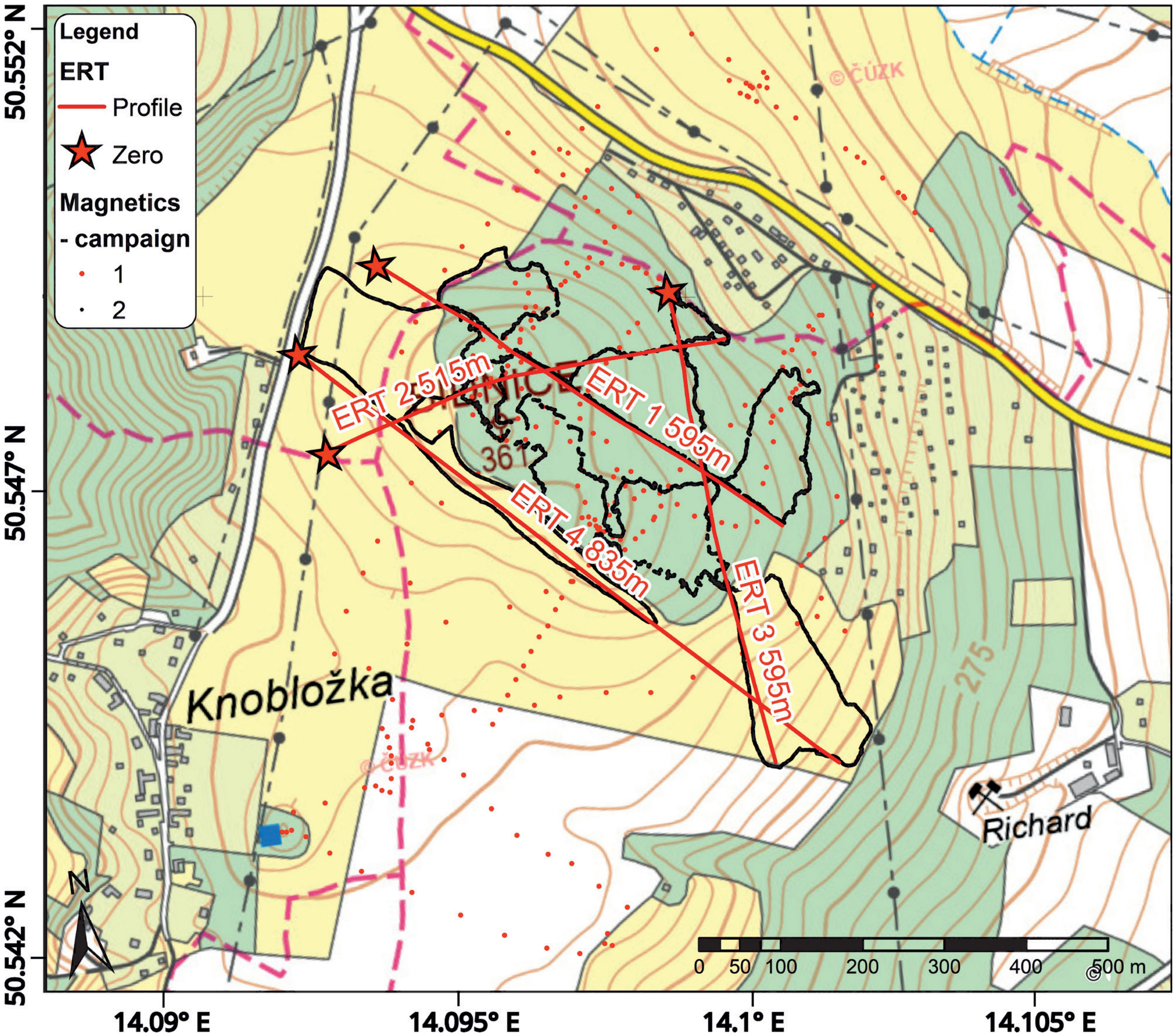

Fig. 2 Four ERT profiles and magnetic data measured over supposed maar-diatreme volcano Bídnice. ERT profiles are displayed as red lines with the profile beginnings (0 m) marked with a star. Magnetic data from the first campaign as red points and from the second campaign as black points. The base map is from State Administration of Land Surveying and Cadastre (https://www.cuzk.cz/en).

magnetic field as they often either amplify or attenuate the magnetic field. Therefore, a ground magnetometry was used mainly to detect coherent mafic volcanic rocks representing the feeder(s) and high-level intrusions within the diatreme breccia. The presence of volcanic rocks should show up as an anomaly in the magnetic field compared to the normal value due to the presence of (ferro- and para-) magnetic minerals in mafic volcanic rocks (e.g., Clark 1999). In total, 293 points covering an area over 0.5 km^2 were measured using a PMG-2 magnetometer (SatisGeo, Brno), with each point georeferenced by a Garmin Oregon GPS receiver (ESM 1). The accuracy of the used magnetometer measurements is 0.1 nT, but the results were rounded to integer numbers (in nT). The daily variations were controlled by repeated measurements on a base point. As the daily variations did not exceed 5 nT, corrections to daily variations were not applied. Additional measurements were carried out later with an aim to improve and verify interpretations of the ERT profiles. For this campaign, a GEM GSM-19GW mobile Overhauser magnetometer with an accuracy of 0.01 nT was used. The sampling frequency was 0.1 Hz. A total of 8028 points were measured in walking mode and georeferenced by a Leica ZENO 20 GNSS receiver with RTK corrections applied (Fig. 2, ESM 1). The variations of the geomagnetic field were, again, observed by repeated measurements on a base point. The variations did not exceed 1 nT in this case and hence no corrections were applied to the final data. The sensor height above the terrain was 2 m in both cases to reduce the artifacts caused by a magnetic debris. The spatial distribution of dT values was then georeferenced and displayed in ArcMap GIS.

3.2. Electrical resistivity tomography

Electrical resistivity tomography (ERT) is designed to detect and distinguish among different lithological, structural and moisture contrasting subsurface bodies based on their distinct geoelectrical properties (usually the higher the water content, the lower the resistivity). Therefore, ERT is often used as a tool for imaging the internal structure of small volcanoes (e.g., Oms et al. 2015; Petronis et al. 2018, 2021). The expected coherent volcanic bodies (dykes, sills, lava flows, etc.) should appear as domains with higher resistivity compared to the surrounding sediments or pyroclastic breccia infill (e.g., Valenta et al. 2014a).

Four ERT profiles with a total length of 2 540 m were measured across Bídnice hill (ESM 2). The location of the profiles was selected with an aim to cross the diatreme margins, with respect to terrain accessibility (see Fig. 2). A dipole-dipole configuration was used for all the profiles, as this measurement geometry provides better resolution of (sub)vertical structures (dykes) (Zhou et al. 2002; Szalai and Szarka 2008; Szalai et al. 2009). In addition, a Wenner-Schlumberger configuration was also measured on profiles 2–4 to better unravel also other, than subvertical boundaries. The electrode spacing was 5 m and the device used was the 5-channel ARES resistivity meter (GF Instruments, ltd.).

Data processing was performed in the RES2DINV software. A standard procedure was used for each profile. First, outlying measurement points with unusually high or low resistivity were removed from the measurements. Next, the appropriate type of inversion (standard - given the expected results), model sensitivity (finest), number of inversions (7), desired RMS error (5%), calculation of the Jacobi matrix for each iteration separately and the full Gauss-Newton method of calculation were selected. From the results, lower iterations were chosen based on the last significant drop of RMS error to avoid excessive inversion artifacts. These models were then displayed with topography and a unified resistivity range for better comparison. Those results were then inserted into ArcMap to correlate them with the diatreme boundary presumed from the elevation map (DMR 5G, a LIDAR based DEM, provided by the State Administration of Land Surveying and Cadastre of the Czech Republic) and a 3D model of the diatreme internal structure was created in MOVE software based on the ERT, magnetic and geological mapping data.

Tab. 1 Whole-rock silicate analysis of Bídnice nepheline sample.

Sample	VRT_R01
Rock	Nephelinite
SiO_2	38.17
TiO_2	2.22
Al_2O_3	12.73
Fe_2O_3	4.64
FeO	7.69
MgO	14.99
CaO	11.22
Na_2O	3.48
K_2O	0.99
P_2O_5	1.156
CO_2	< 0.01
$H_2O(-)$	0.25
Total	100.48

3.3. Petrography and bulk-rock geochemistry

The representative rock sample of a coherent intrusion exposed in the central part of the Bídnice hill (sample VRT-R01, Tab. 1) was thin-sectioned in the labs of the Czech Geological Survey (CGS). The petrography of this sample was then investigated on a Nikon Eclipse LV100N POL polarizing microscopes. The same sample was also used for chemical analysis. Prior to the analytical work, the sample was crushed in steel jaw-crushers and pulverized in an agate mortar. Geochemical analysis was then performed at the Czech Geological Survey, Prague. The major-element analysis followed the methods described by Dempírová et al. (2010) including atomic absorption spectrometry, photometry and titration with Complexon III.

3.4. K–Ar geochronology

The K–Ar age determination of sample VRT-R01 (Tab. 2) was performed in the ATOMKI Laboratories, Debrecen, Hungary. The sieved bulk-rock fraction 0.1–0.3 mm was repeatedly washed in distilled water prior to further analytical procedures. Following acid digestion and 0.2 M HCl dissolution of the samples, the potassium content was determined by flame photometry using a Model 420 Industrial with a Na buffer and Li internal standard. Measurements were checked by inter-laboratory standards (Asia 1/65, LP-6, HD-B1 and GL-O). Argon was extracted from the samples by high-frequency fusion in

Tab. 2 K/Ar dating analyse of Bídnice nepheline sample.

No.	Sample	Atomki no.	Dated fraction	K [%]	$^{40}Ar^*$[ccSTP/g]	r	K/Ar age [Ma]	σ [Ma]
6	VRT-R01	8922	whole rock	0.77	8.20E-07	0.63	27.06	0.57

a Mo crucible under vacuum conditions. A ^{38}Ar-spike was added to samples prior to gas-cleaning in Ti-sponge and SAES St 707 type and liquid nitrogen traps, respectively. The Ar isotope ratios were measured in the static mode using a 15 cm radius magnetic sector-type mass spectrometer built in ATOMKI in Debrecen (see Odin 1982 and Balogh 1985 for details). Age calculations were based on constants proposed by Steiger and Jäger (1977) and the results of K–Ar dating are given with 1σ errors.

3.5. Construction of 3D geological model

The surface geology, magnetic data and ERT results were imported to the MOVE modelling software and used as a basis for the creation of a geological model of the diatreme. The lack of borehole data, reflection seismic or other detailed subsurface information in combination with the complexity of diatreme structure did not allow the creation of the model in a semi-automatic way. The model was then created purely manually by honouring the spatial position and corresponding values of the imported and visualized magnetic and ERT data while following their geological interpretations by the authors. The model is composed of meshes (triangulated irregular networks – TINs) which represent boundaries of dykes, sills and the generalized boundary of the diatreme. The present surface was obtained by interpolation of DEM 5G (DEM data from State Administration of Land Surveying and Cadastre).

4. Results

4.1. Field observations

From a geomorphological point of view, the Bídnice hill is a relatively significant morphological form with an apical plateau elevated some 20 m above the surrounding landscape. The surface of the entire hill was significantly dug up during the II World War due to the creation of anti-aircraft posts protecting the nearby underground factory in the Richard limestone mine and the adjacent field airport between the Bídnice and Radobýl hills. The entire hill is slightly inclined to the NE in general. The regularity of the Bídnice hill shape is interrupted by a smaller depression in the SW subdividing the entire hill into two separate peaks, the Bídnice peak itself (361 m) and a nameless peak to SE (354 m). An agricultural track around the apical part of the Bídnice hill exposes pyroclastic breccia at several sites. The breccia contains frequent fragments of light ochre-coloured porcelanites (thermally metamorphosed marlstones). These sedimentary fragments are derived from the country-rock Cretaceous marine sedimentary rocks and were gathered into

Fig. 3 Olivine nephelinite dike outcrop with well-observable horizontal columnar jointing.

the breccia during volcanic eruptions. These sediments or partially metamorphosed sediments were also found in some pits after the anti-aircraft system relics. Within both peaks, two prominent volcanic dykes of olivine nephelinite with a thickness of up to 7 m were mapped out (Fig. 3), locally with a pronounced columnar jointing with predominantly horizontal orientation. The outcrops of the dykes are limited to only two areas NE from both hill peaks. The first outcrop comes to the surface at the point of intersection with the forest road (a vein belonging to the top of Bídnice) and the second, more massive vein comes to the surface near the gardening settlement (this one is tied to the second top of the hill).

4.2. Magnetometry

The processing of the data included removing of outliers (e.g., caused by artificial metallic objects). Then the measured values of the magnetic field from both campaigns were interpolated to a regular grid using the kriging algorithm implemented in the Golden Software Surfer mapping software (version 25). This process was two-stepped due to the extremely different density of data in both campaigns. In the first step, the data were reduced by taking the median value in 10 × 10 m bins then the reduced data were gridded into the final 20 × 20 m grid. To remove the dipole nature of the magnetic field the differential reduction to pole (RTP) was applied based on the

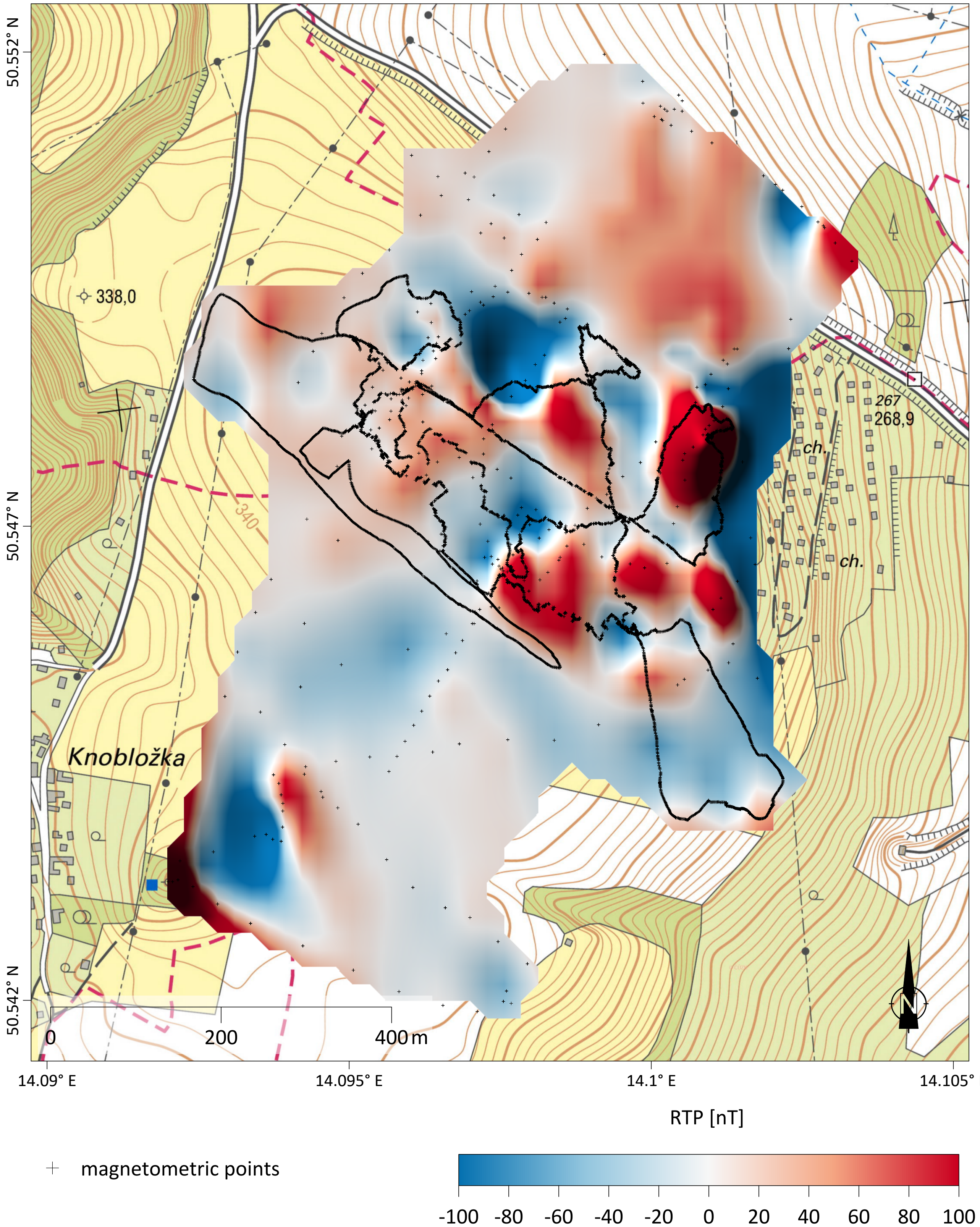

Fig. 4 The geomagnetic survey of the Bídnice diatreme. Plotted are the geomagnetic data reduced to pole (RTP) indicating the mafic volcanic rocks (magnetic highs and lows). Black crosses represent individual magnetic measurements. The base map is provided by the State Administration of Land Surveying and Cadastre (https://www.cuzk.cz/en).

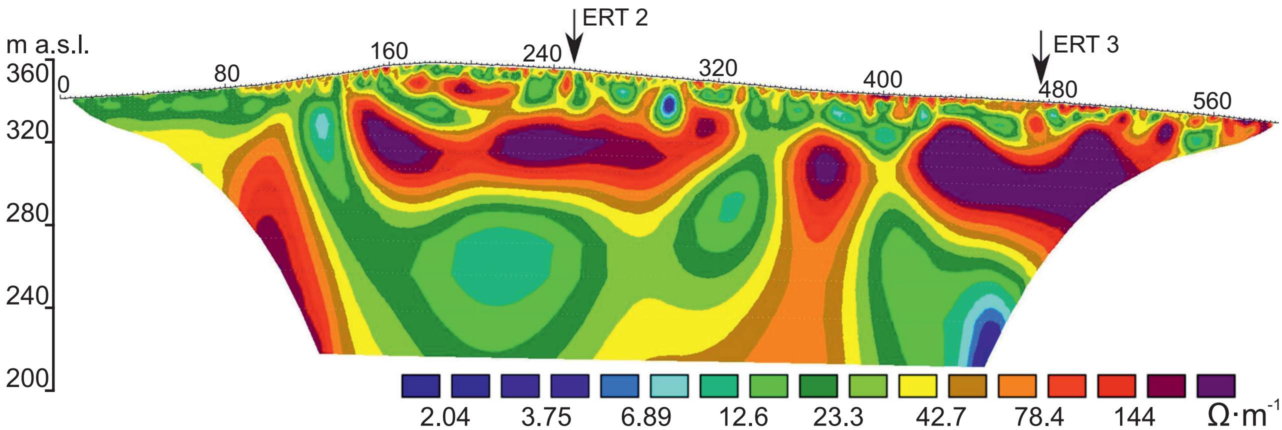

Fig. 5 The resulting model with topography of ERT profile 1 measured with dipole-dipole array. The black arrows show intersections with other profiles.

algorithm by Cooper and Cowan (2005). The final RTP data were plotted as a magnetic map to approximate the position of mafic volcanic conduits and intrusions (Fig. 4), which, unlike pyroclastics and the surrounding Cretaceous sediments, have a much greater effect on the magnetic field (e.g., Skácelová et al. 2010; Valenta et al. 2014a). Three main anomalies were found with the RTP anomaly amplitude exceeding 1500 nT (more than 7000 nT in the raw dataset).. Several smaller anomalies were observed with lower amplitudes (±300 nT) compared to the first four, but in general also significant (e.g., Mrlina et al. 2009; Petronis et al. 2021; Valenta et al. 2014a).

4.3. Electrical resistivity tomography

The results show complex images with significant variations in resistivities, suitable for further geological interpretations.

The results of the profile 1 (Fig. 5) show vertical high-resistivity structures around 80–120 m and 350–390 m, and horizontally oriented high-resistivity spoon-shaped structures around 140–330 m and 420–520 m with low-resistivity zones underneath them.

The computed model derived from the profile 2 (Fig. 6) shows a higher-resistivity vertical structure between 90 and 140 m, probably a subvertical structure between 420 and 470 m and three subhorizontal structures around 180–240 m, 240–290 m and 290–390 m. The space between vertical structures and underneath subhorizontal structures has low resistivity. Both profiles 1 and 2 show comparable results at given depths near their intersection.

The resulting model of the profile 3 (Fig. 7) shows a similar image to profile 1, as it contains two vertical high-resistivity anomalies, a horizontal high-resistivity anomaly with low resistivity underneath. The first vertical anomaly is found around 100–140 m, the second

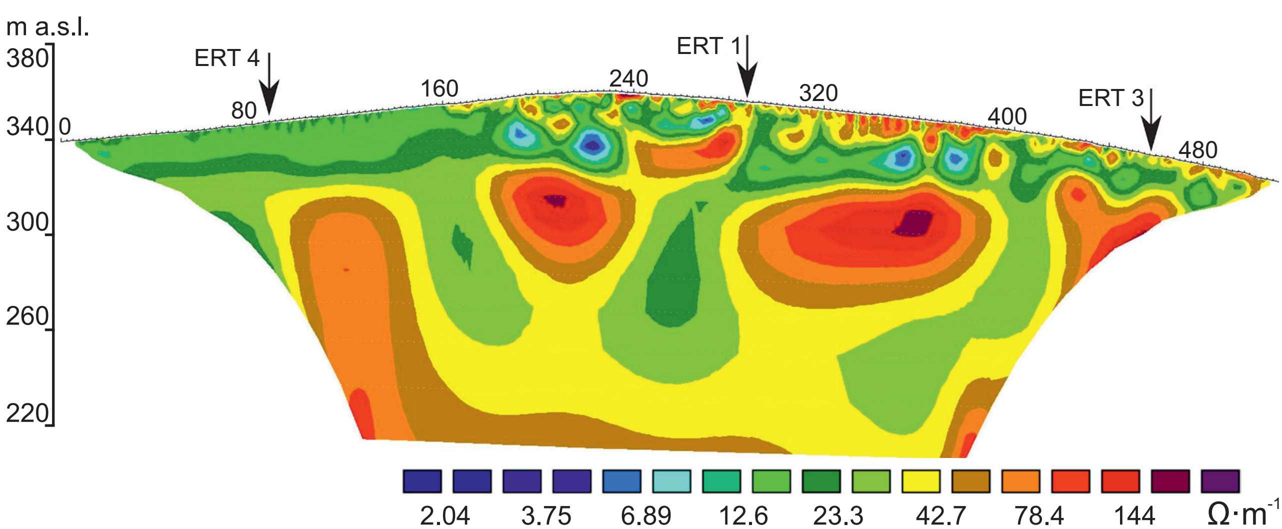

Fig. 6 The resulting model with topography of ERT profile 2 measured with dipole-dipole array. The black arrows show intersections with other profiles.

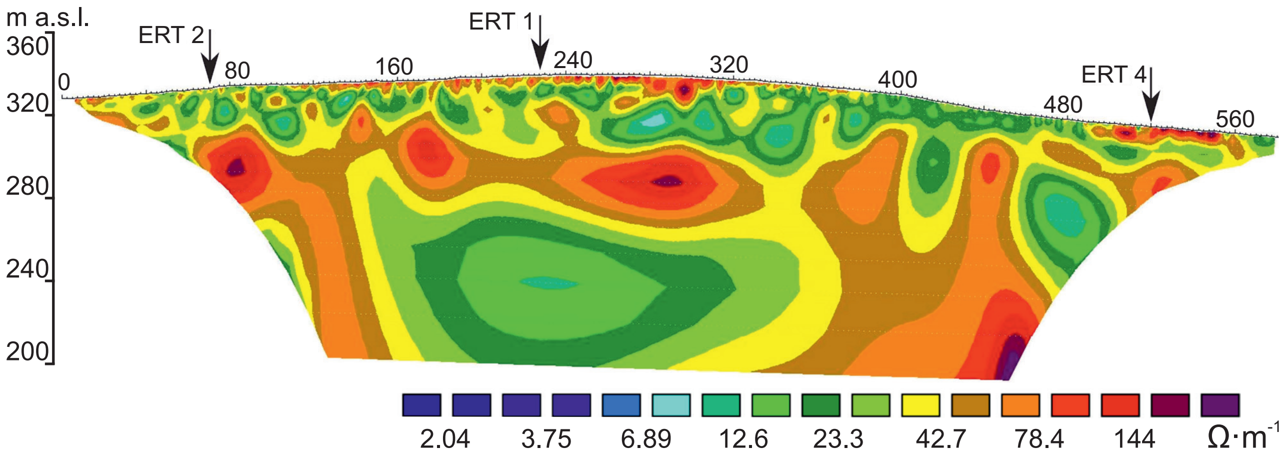

Fig. 7 The resulting model with topography of ERT profile 3 measured with dipole-dipole array. The black arrows show intersections with other profiles.

430–460 m and a spoon-like horizontal structure between them with a lower resistivity zone underneath. Note the similar results at the intersection with profiles 1 and 2.

The last measured ERT profile was chosen to try to capture both diatremes of the volcano from the other side of profile 1 with respect to the limited terrain accessibility. The profile (Fig. 8) shows two higher-resistivity structures, the first between 80 and 340 m, which corresponds with the vertical structure in profile 2, and the second between 440 and 670 m. The results also show a small higher-resistivity vertical structure near the surface at 400 m with an adjacent low-resistivity structure at 420 m and a horizontal high-resistivity structure between 510 m and the end of the profile.

4.4. Petrography and geochronology

Olivine nephelinite of the intrusion exposed in the central part of the diatreme is finely porphyritic and fine-grained, not displaying any preferred orientation. The phenocrysts are dominated by olivine (up to 3 mm, Fig. 9) with subordinate clinopyroxene (not exceeding 1.5 mm). Optical zonality of the clinopyroxene phenocrysts is well developed.

The rock groundmass consists mainly of clinopyroxene (40 vol. %), which has a maximum size of 0.2 mm, with automorphic to hypautomorphic shape and do not display preferred orientation. The second most abundant mineral (ca 35 vol. %) is nepheline reaching up to 0.3 mm, represented mostly by intersticial grains. The last matrix mineral (25 vol. %) is an automorphic to hypautomorphic Fe–Ti oxide, most-probably represented by the magnetite–ulvöspinel solid-solution. The only accessory mineral found is apatite forming very small (up to 100 μm long) needles in the groundmass. The sample does not contain any vesicles, traces of volcanic glass or secondary carbonate or zeolite mineralization.

The rock is classified as foidite in the TAS diagram (Fig. 10), accordingly to the abundant nepheline in the

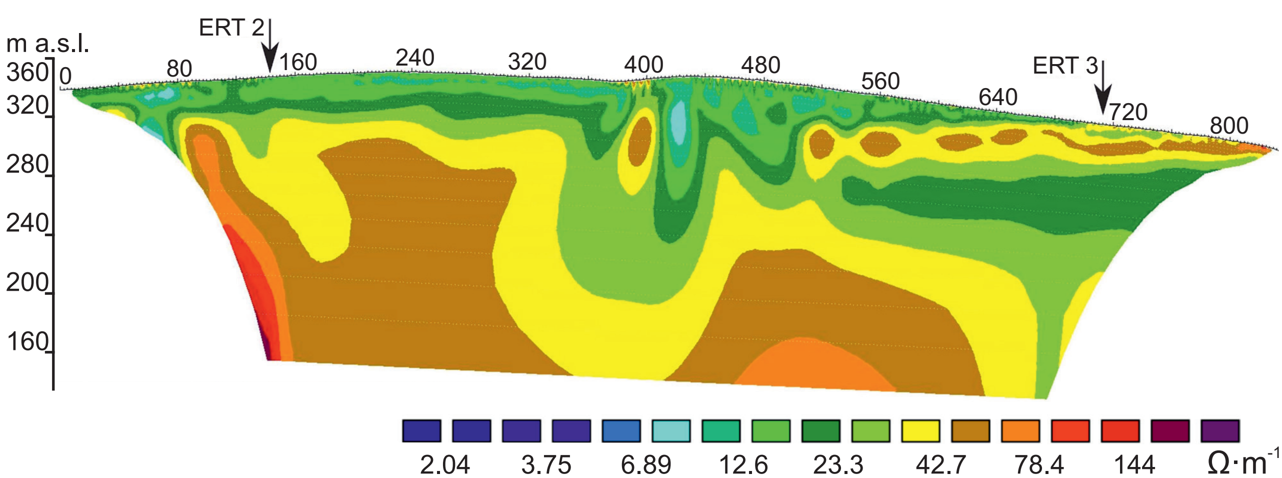

Fig. 8 The resulting model with topography of ERT profile 4 measured with dipole-dipole array. The black arrows show intersections with other profiles.

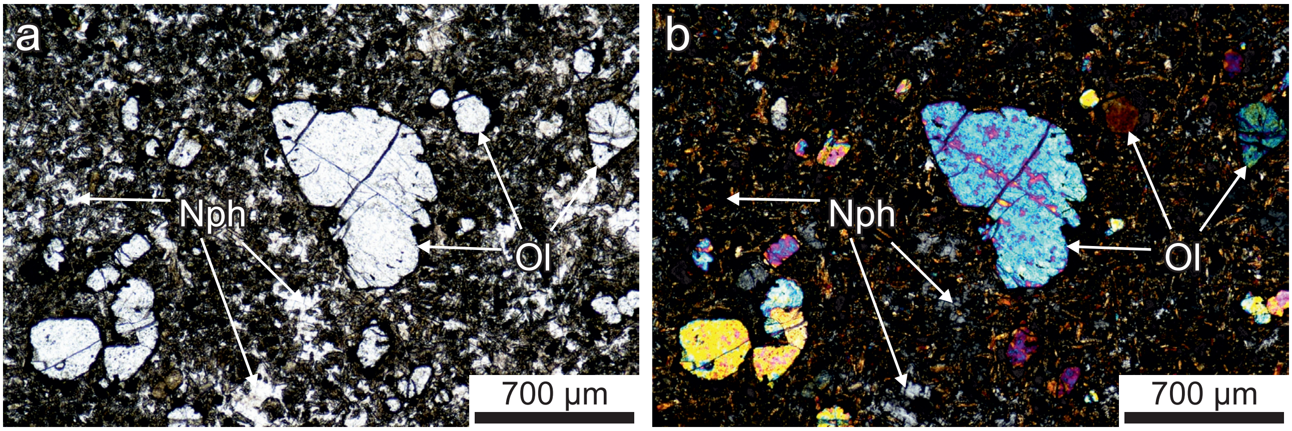

Fig. 9 Olivine nephelinite from Bídnice diatreme in thin section. 9a (/N), 9b (XN). Nph = nephelinite, Ol = olivine (abbreviations by Whitney and Evans 2010).

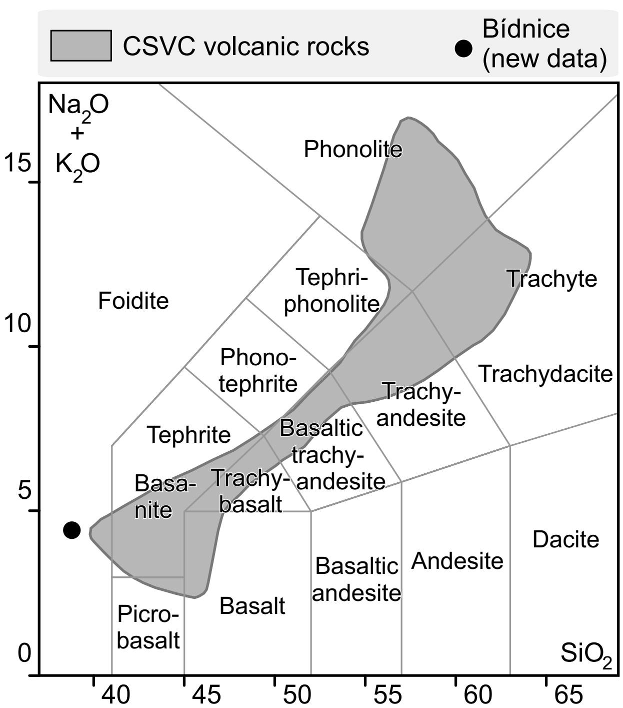

Fig. 10 Classification of the studied rocks in TAS diagram (Le Maitre et al. 2002). Data from České Středohoří Volcanic Complex (Ulrych et al. 2002; Ackerman et al. 2015; Mysliveček et al. 2018).

groundmass. Compared to other common volcanic rocks of the CSVC (see Cajz et al. 1999; Ulrych et al. 2002), the olivine nephelinite from the Bídnice hill is characterized by even lower SiO_2 content (38.17 wt. %), combined with elevated MgO (14.99 wt. %), which is reflected also in the high Mg# value (69).

The rock sample was analysed in the ATOMKI laboratory using the K/Ar dating method. The sample provided age of 27.06 ± 0.57 Ma (Oligocene). The low-silica, high MgO and abundant presence of olivine phenocrysts classify this occurrence as the intrusive equivalent of the Ústí Fm. (sensu Cajz et al. 1999).

4.5. 3D model of the diatreme interior

The model (Fig. 11 and 12) consists of 3 major components – boundary of the diatreme, feeder dykes and spoon-shaped sills. The diatreme boundary on the surface follows the results of ERT, magnetic and geological mapping. The deeper parts of the diatreme boundary were created as an expert estimate based on knowledge of other diatremes in the wider area (e.g., Skácelová et al. 2010), because no data are available from depth that could be used for estimating the dip of the Bídnice double-funnel walls.

Feeder dykes were constructed in regions with the highest magnetic anomalies and surface outcrops of compact basalt, using detailed knowledge of the geometry of one of the basaltic feeder dykes that is well exposed on the surface further to the SW where it was also reached on many places in the nearby underground Richard limestone mine. The basaltic sills were created purely on the basis of the ERT data, assuming that the relatively thin flat sheet of basalts cannot induce any significant magnetic anomaly.

5. Discussion

From the magnetometry results (Fig. 4) in our area of interest, we can see two major anomaly zones in the central and eastern parts of the map, which according to their amplitude and geometry most likely represent basaltic dykes, one intruded into the diatreme and the other outside, as the vertical and subvertical basaltic structures show high anomalies directly above them, whereas sills show lower anomalies over a larger area. Anomalies reaching up to ca 7000 nT are not common in the Bohemian Cretaceous Basin sediments but are frequently associated with basaltic feeders (Šalanský and Gnojek 2002). Several other zones with higher anomalies (dT

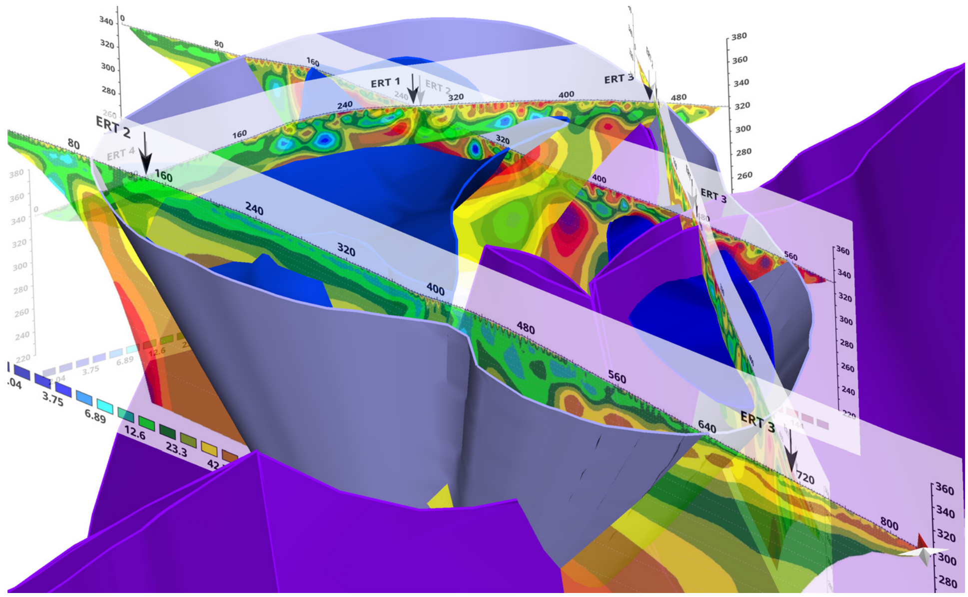

Fig. 11 3D model of Bídnice peanut-shaped diatreme with modelled nephelinite dykes and spoon-like nephelinite sills with embedded results from geophysical survey.

above 300 nT) can be seen in the northern part near ERT profiles 1 and 2, near the intersection of profiles 1 and 3 and at the SE unnamed peak. Those, along with other minor anomalies are probably effects of sills, breccia and other volcanoclastic material. The highest anomalies are often found in places with outcrops of olivine nephelinite. The magnetometry therefore indicates that Bídnice is a structure of volcanic origin comprising a feeding system of rocks with higher amount of ferromagnetic minerals (usually basalts).

The structure of the studied volcanic body can be also identified on individual profiles using electrical resistivity measurements. From the results of the four ERT profiles, we can observe that the resistivities of rocks under the hilltop are often lower than those that represent the surrounding Cretaceous sediments, as well as coherent volcanic bodies verified on the surface or by the magnetometric survey. From these findings we can assume, that those lower resistivities are caused by breccia of disrupted country rocks filling the diatreme. In turn it implies that Bídnice is a deeply eroded maar-diatreme volcano.

On the ERT profile 1 (Fig. 5) the diatreme boundaries are probably around 120 m and maybe near the end of the profile at 550 m corresponding with subvertical low-resistivity anomalies. The high-resistivity horizontal spoon-like structure between 140 and 330 m, which is similar to a sill in diatreme described by Valentine and van Wyk de Vries (2014) most likely corresponds to a spoon-shaped sill. The second horizontal high-resistivity structure between 420–520 m could also be a sill. The low-resistivity zones beneath the mentioned horizontal structures are probably country rocks filling the diatreme with the other low-resistivity anomalies representing colluvial deposits and pyroclastic breccias. The vertical high-resistivity structure around 370 m might represent a dyke.

The ERT profile 2 (Fig. 6) shows three similar higher-resistivity horizontal structures at 180–240 m, 240–290

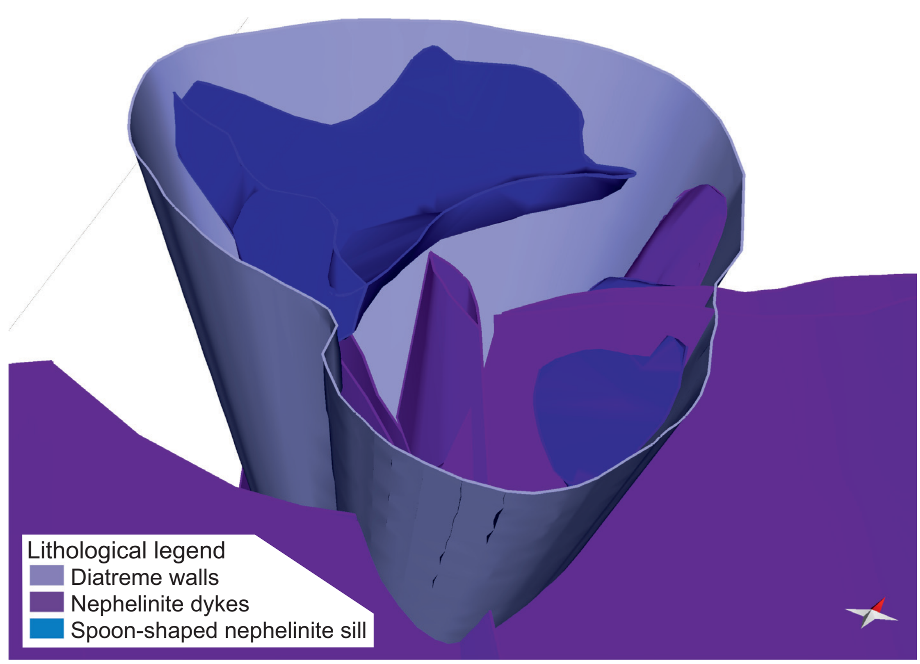

Fig. 12 3D model of Bídnice peanut-shaped diatreme with modelled nephelinite dykes and spoon-like nephelinite sills.

m and 290–390 m. The two low-resistivity subvertical zones around 140 and 410 m could probably be the edges of the diatreme. Along this profile, the average resistivities between these edges show a diatreme fill, without significant indications of any feeder dyke.

The next measured ERT profile 3 (Fig. 7) is consistent with the results of profiles 1 and 2 as it also probably crossed both walls of the diatreme (low-resistivity vertical anomalies). The profile enters the diatreme around 60 m with a sill lying along the wall (confirmed by magnetometry). The wall is not so evident from ERT results, as there is insufficient depth coverage at the edge of the profile, but it is assumed based on the shape of the mentioned sill. The diatreme was then left by the profile around 430 m. The high-resistivity horizontal zone at around 150–400 m is probably a similar spoon-like structure with lower extent. The low resistivities underneath this structure probably represents the diatreme fill.

The last profile 4 (Fig. 8) caught the spoon like structure (and the diatreme) only peripherally at around 80–410 m, because the resistivity values representing it are lower and the magnetometry results along the profile shows no sign of magnetic rocks. The two significant vertical low-resistivity zones around 60–80 m and 400–440 m represent the edges of the diatreme with the high-resistivity anomaly around 440–670 m probably being the wall of the second diatreme. From these results it seems that the SE diatreme is probably older, as it doesn't show a cone cylinder in the results opposed to the NW diatreme and the margin of the NW diatreme most likely cross-cuts the SE diatreme (Fig. 13).

The mafic and silica-poor geochemical character of the magma in combination with the low content of phenocrysts correspond to rather low effective viscosity, enabling easy injection of the melt into the surrounding breccias during ascent. It appears from the geophysical measurements that this magma was suitable for the formation of relatively thin sills, in contrast to the differentiated alkaline (phonolitic) magmas emplaced also in diatremes in other parts of the Ohře Rift (e.g., Bořeň: Závada et al. 2011; Luž: Wenger et al. 2017; Rapprich et al. 2022). Phonolitic intrusions/extrusions emplaced into the maar-diatreme volcanoes tend to form a positive morphology already during the volcanic activity. In addition, the high resilience of phonolite against erosion lead to reshaping of such structures into significant morphological peaks. On the other hand low-viscosity magma does not form such high aspect-ratio volcanic bodies attenuating significant morphology. The reason of the Bídnice maar-diatreme volcano having a positive relief could be the level of erosion, as a presumed upper bedded part of the diatreme could be already eroded, and the current surface level might represent the transition zone between the lower and upper diatreme facies (*sensu* Lorenz 2003) which is probably hardened by dykes and sills evidenced from geophysical survey. Therefore, the surrounding sedimentary rocks were eroded faster than the diatreme fill.

Additionally, the present diatreme might also be hardened by the spoon-like structures found by ERT measurements and modelled in MOVE software (Fig 11 and 12). In that case, considering the extent (diameter) and shape (concavity) of these intrusions, it is matching the inward dipping bedded breccia of upper diatreme facies (Lorenz 2003) and recent results of diatreme modelling including basaltic intrusions (Almaguer et al. 2023). Therefore, we can assume that the sills have intruded either at the lower/upper diatreme boundary or into the upper diatreme, which is characterized by the inward-dipping bedding.

In case the diatreme was hardened only by dykes, it would be rather eroded like other occurrences in this area, for instance, further to the SW (Bílé Stráně u Malíče). Here the erosion-exposed dykes form

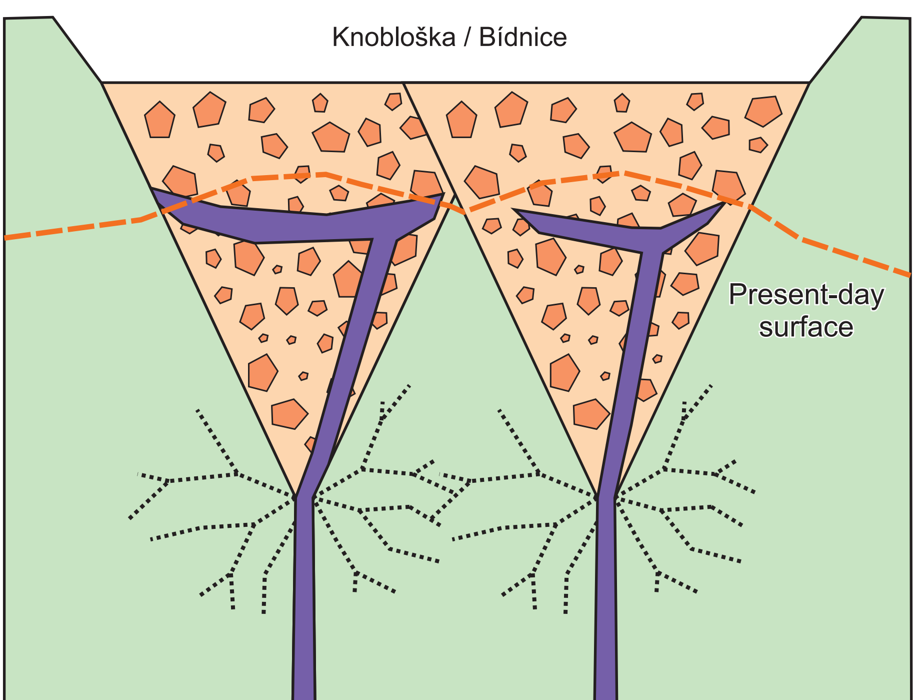

Fig. 13 Diatreme schemes with present surface indicated. The picture is not to scale and serves just as an illustration.

steep hills with outcrops on top. By having a spoon-shaped structure, the whole Bídnice diatreme resists erosion and forms a gentle hill rather than a sharp peak as illustrated in the scheme in Fig. 13.

6. Conclusions

Based on a thorough geophysical survey, a new peanut-shaped (twinned-funnel) diatreme was identified at the southern margin of the České Středohoří Volcanic Complex, which led to the characterization of the Bídnice hill as a deeply eroded maar-diatreme volcano. The sample of coherent olivine nephelinite dyke from this diatreme was dated using the K/Ar method to 27.06 ± 0.57 Ma.

The elevated morphological form, which is atypical for diatreme volcanoes, might be caused by the relatively large spoon-shaped intrusions found by the geophysical survey at a depth around 20–30 m below the present surface. The intrusions harden the whole diatreme structure making it less prone to erosion, therefore causing the positive relief.

The model of the volcanic structure along with the spoon-shaped intrusions was manually constructed in MOVE software based on georeferenced results from ERT and magnetometry, DMR 5G (DEM data from State Administration of Land Surveying and Cadastre) and field observations for a more precise interpretation and better visualization of the results. This model is then intended for easy visual comparison with results of further studies of inverse relief and the internal structure of diatremes elsewhere.

Acknowledgements: The geophysical survey was carried out within the framework of the Interreg project "Cross-border cooperation for the development of railway traffic Saxony – Czech Republic". The research contributes to the Strategic Research Plan of the Czech Geological Survey (DKRVO/ČGS 2023–2027, internal grant 321560). We gratefully acknowledge the critical reviews by two anonymous reviewers and the editorial handling by A. Guy.

Electronic supplementary material. Supplementary material to this paper, including raw geophysical survey results and a video overview of the diatreme model is available online at the Journal web site *(http://dx.doi.org/10.3190/jgeosci.396)*.

References

Ackerman L, Ulrych J, Řanda Z, Erban V, Hegner E, Magna T, Balogh K, Frána J, Lang M, Novák JK (2015) Geochemical characteristics and petrogenesis of phonolites and trachytic rocks from the České Středohoří Volcanic Complex, the Ohře Rift, Bohemian Massif. Lithos 224–225: 256–271

Almaguer J, Guevara-Betancourt R, Sieck P, Aguillón-Robles A, Lopez-Loera H, Cerca-Ruiz MF, Tristán-González M (2023) An integrated geophysical and geological 3D model to characterize the feeder system of La Joya Honda and La Joyuela maars complex in central Mexico. J South Am Earth Sci 125: 104254

Babuška V, Plomerová J (1992) The lithosphere in central Europe – seismological and petrological aspects. Tectonophysics 207: 141–163

Babuška V, Plomerová J (2001) Subcrustal lithosphere around the Saxothuringian–Moldanubian Suture Zone – a model derived from anisotropy of seismic wave velocities. Tectonophysics 332: 185–199

Babuška V, Plomerová J (2010) Mantle lithosphere control of crustal tectonics and magmatism of the western Ohře (Eger) Rift. J Geosci 55: 171–186

Balogh K (1985) K/Ar Dating of Neogene Volcanic Activity in Hungary: Experimental Technique, Experiences and Methods of Chronologic Studies. ATOMKI Reports D/1: 277–288

Cajz V, Vokurka K, Balogh K, Lang M, Ulrych J (1999) The České Středohoří Mts.: volcanostratigraphy and geochemistry. Geolines 9: 21–28

Cajz V, Rapprich V, Erban V, Pécskay Z, Radoň M (2009) Late Miocene volcanic activity in the České Středohoří mountains (Ohře/Eger Graben, northern Bohemia). Geol Carpath 60: 519–533

Clark DA (1999) Magnetic petrology of igneous intrusions: implications for exploration and magnetic interpretation. Exploration Geophysics 30(2): 5–26

Cooper GRJ, Cowan DR (2005) Differential reduction to the pole. Comp Geosci 31: 989–999

Dempírová L, Šikl J, Kašičková R, Zoulková V, Kříbek B (2010) The evaluation of precision and relative error of the main components of silicate analyses in Central Laboratory of the Czech Geological Survey. Geoscience Research Reports for 2009: 326–330 (in Czech)

Domas S (ed 1988) Geological map of the Czech Republic, sheet 02-43 Litoměřice. Czech Geological Survey, Prague

Fodor L, Csillag G, Németh K, Budai T, Cserny T, Martin U, Brezsnyászky K, Dewey J (2005) Tectonic development, morphotectonics and volcanism of the Transdanubian Range: a field guide. Occasional Papers of the Geological Institute of Hungary 204: 59–86

Gebhardt AC, De Batist M, Niessen F, Anselmetti FS, Ariztegui D, Haberzettl T, Kopsch C, Ohlendorf C, Zolitschka B (2011) Deciphering lake and maar geometries from seismic refraction and reflection surveys in Laguna Potrok Aike (southern Patagonia, Argentina). J Volcanol Geotherm Res 201: 357–363

Graettinger AH, Bearden AT (2021) Lateral migration of explosive hazards during maar eruptions constrained from crater shapes. J Appl Volcanol 10: 1–14

Goes S, Spakman W, Bijwaard H (1999) A lower mantle source for central European volcanism. Science 286: 1928–1931

Hencz M, Németh K, Spránitz T, Biró T, Karátson D, Berkesi M (2024) Evolution and polycyclic nature of a maar-diatreme volcano as constrained by changing external factors. J Volcanol Geotherm Res 453: 108158

Holub FV, Rapprich V, Erban V, Pécskay Z, Mlčoch B, Míková J (2010) Petrology and geochemistry of the Tertiary alkaline intrusive rocks at Doupov, Doupovské hory Volcanic Complex (NW Bohemian Massif). J Geosci 55: 251–278

Hoernle K, Zhang YS, Graham D (1995) Seismic and geochemical evidence for large-scale mantle upwelling beneath the eastern Atlantic and western and central Europe. Nature 374: 34–39

Hošek J, Valenta J, Rapprich V, Hroch T, Turjaková V, Tábořík P, Pokorný P (2019) Newly identified Pleistocene maars in Western Bohemia (Czech Republic). Geosci Res Reports 52(2): 97–104

Hrubcová P, Fischer T, Rapprich V, Valenta J, Tábořík P, Mrlina J, Dahm T, Vylita T, Beránek R, Klanica R, Turjaková V (2023) Two small volcanoes, one inside the other: Geophysical and drilling investigation of Bažina maar in western Eger Rift. Earth Space Sci 10: e2023EA003009

Jung S, Pfänder J, Braus M, Maas R (2011) Crustal contamination and mantle source characteristics in continental intra-plate volcanic rocks: Pb, Hf and Os isotopes from central European volcanic province basalts. Geochim Cosmochim Acta 75: 2664–2683

Latutrie B, Ross Ps (2019) Transition zone between the upper diatreme and lower diatreme: origin and significance at Round Butte, Hopi Buttes volcanic field, Navajo Nation, Arizona. Bull Volcanol 81: 1–22

Le Maitre RW, Streckeisen A, Zanettin B, Le Bas MJ, Bonin B, Bateman P, Bellieni G, Dudek A, Efremova S, Keller J, Lamavre J, Sabine Pa, Schmid R, Sørensen H, Wooley AR (2002) Igneous Rocks. A Classification and Glossary of Terms. Recommendations of the International Union of Geological Sciences Subcommission on the Systematics of Igneous Rocks, 2nd Edition. Cambridge University Press, Cambridge–New York, pp 1–193

Lorenz V (2003) Maar-diatreme volcanoes, their formation, and their setting in hard-rock or soft-rock environments. Geolines 15: 72–83

Lustrino M, Wilson M (2007) The circum-Mediterranean anorogenic Cenozoic igneous province. Earth Sci Rev 81: 1–65

Mlčoch B, Konopásek J (2010) Pre-Late Carboniferous geology along the contact of the Saxothuringian and Teplá–Barrandian zones in the area covered by younger sediments and volcanics (western Bohemian Massif, Czech Republic). J Geosci 55: 81–94

Mrlina J, Kämpf H, Kroner C, Mingram J, Stebich M, Brauer A, Geissler WH, Kallmeyer J, Matthes H, Seidl M (2009) Discovery of the first Quaternary maar in the Bohemian Massif, Central Europe, based on combined geophysical and geological surveys. J Volcanol Geotherm Res: 182, 97–112

Mysliveček J, Rapprich V, Kochergina YV, Magna T, Halodová P, Pécskay Z, Poňavič M (2018) Petrology of weakly differentiated alkaline, high-level intrusive rocks in the Zahořany–Chotiněves Belt near Litoměřice (Czech Republic). J Geosci 63: 317–331

Németh K, Martin U, Harangi S (2001) Miocene phreatomagmatic volcanism at Tihany (Pannonian Basin, Hungary). J Volcanol Geotherm Res 111: 111–135

Németh K, Martin U, Csillag G (2007) Pitfalls in erosion level calculation based on remnants of maar and diatreme volcanoes. Géomorphologie relief processus environnement 13: 225–236

Odin GS (1982) Numerical Dating in Stratigraphy. John Wiley and Sons, New York, pp 1–1040

Oms O, Bolós X, Barde-Cabusson S, Martí J, Casas A, Lovera R, Himi M, Gómez De Soler B, Campeny Vall-Llosera G, Pedrazzi D, Agustí J (2015) Structure of the Pliocene Camp dels Ninots maar-diatreme (Catalan Volcanic Zone, NE Spain). Bull Volcanol 77: 1–13

Petronis MS, Valenta J, Rapprich V, Lindline J, Heizler M, Van Wyk De Vries B, Shields S, Balek J, Fojtíková L, Tábořík P (2018) Emplacement History of the Miocene Zebín Tuff Cone (Czech Republic) Revealed From Ground Geophysics, Anisotropy of Magnetic Susceptibility, Paleomagnetic, and $^{40}Ar/^{39}Ar$ Geochronology Data. Geochem Geophys Geosyst 19: 3764–3792

Petronis MS, Awdankiewicz M, Valenta J, Rapprich V, Zebrowski JP, Karim E (2021) Eruptive and magma feeding system evolution of Sośnica Hill Volcano (Lower Silesia, SW Poland) revealed from Volcanological, Geophysical, and Rock Magnetic Data. J Volcanol Geotherm Res 419: 107367

Rapprich V, Büchner J, Skácelová Z, Tietz O, Pour O (2022) Complements to the volcanic history of Luž/Lausche Volcano. Z Dtsch Ges Geowiss 173: 345–355

Šalanský K, Gnojek I (2002) Geomagnetic anomalies in the Czech Republic. Czech Geological Survey, pp 1–141 (in Czech with English resume)

Schulz R, Buness H, Gabriel G, Pucher R, Rolf C, Wiederhold H, Wonik T (2005) Detailed investigation of preserved maar structures by combined geophysical surveys. Bull Volcanol 68: 95–106

Skácelová Z, Rapprich V, Valenta J, Hartvich F, Šrámek J, Radoň M, Gaždová R, Nováková L, Kolínský P, Pécskay Z (2010) Geophysical research on structure of partly eroded maar volcanoes: Miocene Hnojnice and Oligocene Rychnov volcanoes (northern Czech Republic). J Geosci 55: 333–345

Steiger RH, Jäger E (1977) Subcommission on Geochronology; convention on the use of decay constants in geo and cosmochronology. Earth Planet Sci Lett 36: 359–362

Szalai S, Szarka L (2008) Parameter sensitivity maps of surface geoelectric arrays. Part 1: linear arrays. Acta Geod Geophys Hung 43: 419–437

Szalai S, Novák A, Szarka L (2009) Depth of investigation and vertical resolution of surface geoelectric arrays. J Environ Eng Geophys 14: 15–23

Ulrych J, Pivec E, Lang M, Balogh K, Kropáček V (1999) Cenozoic intraplate volcanic rock series of the Bohemian Massif: a review. Geolines 9: 123–129

Ulrych J, Svobodová J, Balogh K (2002) The source of Cenozoic volcanism in the České středohoří Mts., Bohemian Massif. Neu Jb Mineral, Abh 177: 133–162

Ulrych J, Dostál J, Adamovič J, Jelínek E, Špaček P, Hegner E, Balogh K (2011) Recurrent Cenozoic volcanic activity in the Bohemian Massif (Czech Republic). Lithos 123: 133–144

Valenta J, Rapprich V, Stárková M, Skácelová Z, Fojtíková L, Staněk F, Balek J (2014a) Problems and challenges in detection of pre-Mesozoic maar volcanoes: example from the Principálek Volcano in the Permian Krkonoše Piedmont Basin. J Geosci 59: 169–181

Valenta J, Rapprich V, Skácelová Z, Gaždová R, Fojtíková L (2014b) The newly discovered Neogene maar volcano near the Mariánské Lázně, Western Bohemia. Acta Geodyn Geomater 11: 107–116

Valentine GA, Van Wyk De Vries B (2014) Unconventional maar diatreme and associated intrusions in the soft sediment-hosted Mardoux structure (Gergovie, France). Bull Volcanol 76: 1–16

Van Wyk De Vries B, Karatson D, Gouard C, Németh K, Rapprich V, Aydar E (2022) Inverted volcanic relief: Its importance in illustrating geological change and its geoheritage potential. Int J Geoheritage Parks 10: 47–83

Wedepohl KH, Baumann A (1999) Central European Cenozoic plume volcanism with OIB characteristics and indications of a lower mantle source. Contrib Mineral Petrol 136: 225–239

Wenger E, Büchner J, Tietz O, Mrlina J (2017) The polycyclic Lausche Volcano (Lausitz Volcanic Field) and its message concerning landscape evolution in the Lausitz Mountains (northern Bohemian Massif, Central Europe). Geomorphology 292: 193–210

White JDL, Ross PS (2011) Maar-diatreme volcanoes: a review. J Volcanol Geotherm Res 201: 1–29

White JDL, Valentine GA (2016) Magmatic versus phreatomagmatic fragmentation: Absence of evidence is not evidence of absence. Geosphere 12: 1478–1488

Whitney DL, Evans BW (2010) Abbreviations for names of rock-forming minerals. Amer Miner 95: 185–187

Wilson M, Downes H (1991) Tertiary Quaternary extension-related alkaline magmatism in Western and Central Europe. J Petrol 32: 811–849

Závada P, Dedecek P, Mach K, Lexa O, Potuzak M (2011) Emplacement dynamics of phonolite magma into maar-diatreme structures – Correlation of field, thermal modelling and AMS analogue modelling data. J Volcanol Geotherm Res 201: 210–226

Zhou W, Beck BF, Adams AL (2002) Effective electrode array in mapping karst hazards in electrical resistivity tomography. Environ Geol 42: 922–928